Efficient synthesis of furfural from xylose over HCl catalyst in slug flow microreactors promoted by NaCl addition

Guo, Wenze; Bruining, Herman; Heeres, Hero; Yue, Jun

Published in:
AIChE Journal

DOI:
10.1002/aic.17606

Publication date:
2022

Received: 23 October 2021 | Revised: 29 December 2021 | Accepted: 9 January 2022

DOI: 10.1002/aic.17606

AIChE JOURNAL

RESEARCH ARTICLE

Reaction Engineering, Kinetics and Catalysis

Efficient synthesis of furfural from xylose over HCl catalyst in slug flow microreactors promoted by NaCl addition

Wenze Guo | Herman Carolus Bruining | Hero Jan Heeres | Jun Yue

Department of Chemical Engineering, Engineering and Technology Institute Groningen, University of Groningen, Groningen, The Netherlands

Correspondence
Jun Yue, Department of Chemical Engineering, Engineering and Technology Institute Groningen, University of Groningen, Nijenborgh 4, 9747 AG Groningen, The Netherlands.
Email: yue.jun@rug.nl

Funding information
China Scholarship Council, Grant/Award Number: 201606740069; Rijksuniversiteit Groningen

Abstract

Efficient synthesis of furfural from xylose over the HCl catalyst in a water-methyl isobutyl ketone biphasic system was achieved in slug flow microreactors, using NaCl as a promotor which facilitates xylose dehydration and suppresses xylose condensation. An optimized furfural yield of 93% was obtained from 1 M xylose over 0.2 M HCl with 10 wt% NaCl at 180°C within 4 min. A comprehensive kinetic model was developed from monophasic experiments in water in microreactors, by incorporating the acidity in water and kinetic constants as a function of the chloride ion concentration. The coupling of kinetic model with furfural extraction, with consideration of phase volume change as a function of temperature and partial phase miscibility, enables to predict the results of biphasic experiments in microreactors where mass-transfer limitation was eliminated. The aqueous phase containing HCl and NaCl could be readily recycled and reused multiple times without noticeable performance loss.

KEYWORDS
Brønsted acid, furfural, kinetics, microreactor, sodium chloride

1 | INTRODUCTION

Transformation of biomass into chemicals and fuels offers vast opportunities towards developing a green and sustainable chemical industry.[1,2] Currently, the conversion of lignocellulose-derived carbohydrates to bio-based platform chemicals has attracted significant attention.[3] One such carbohydrate is xylose, the most abundant pentose produced by hydrolysis of the hemicellulosic fraction of lignocellulose (25%–35% on a dry basis).[4] Xylose can be dehydrated to furfural, a versatile platform chemical for synthesizing a variety of bio-based fuels, chemicals, and polymers.[5] For example, furfural can be converted via hydrogenation to furfuryl alcohol (monomer of furan resins), tetrahydrofuran (widely used industrial specialty solvents), 2-methylfuran and 2-methyltetrahydrofuran (both as the potential transportation fuel additives).[5,6] Recently, photo-oxidation of furfural to hydroxybutenolide was reported, which can be further etherified to alkoxybutenolide (a promising bio-based monomer to produce high-performance coatings).[7] Furthermore, via a series of aldol condensation and dehydration/hydrogenation reactions, furfural can be transformed into liquid alkanes for use as gasoline, diesel, or aviation fuel.[8]

Xylose dehydration is typically performed in water over homogeneous Brønsted acid catalysts (e.g., sulfuric, hydrochloric, and formic acids) with a furfural yield of ca. 40%–60%.[9] The reaction network usually involves xylose dehydration to furfural, xylose condensation and furfural degradation to humins (soluble or insoluble carbonaceous polymers).[9] One strategy to improve the furfural yield is suppressing side reactions involving furfural by its in situ extraction or stripping from aqueous reaction media. The first industrial process for furfural production was established in 1921 by Quaker Oats Company, where oat hulls were converted to furfural using the dilute H_2SO_4 catalyst and water steam to supply heat and strip out furfural.[10] So far, the industrial furfural production is still conducted in similar energy-intensive processes over homogeneous acid catalysts using batch or

continuous reactors.[11] However, these processes are inefficient with ca. 50% furfural yield. Recently, high research attention has been given to developing the aqueous-organic biphasic solvent systems for furfural synthesis, where furfural formed in the aqueous reaction phase was extracted to a nonreactive organic solvent to prevent its further degradation.[6,9] However, most reactions in biphasic systems were conducted in lab-scale batch reactors with the dilute feedstock (ca. 1 wt% xylose) and extended reaction time (ca. 1 h or more), leading to a limited space-time yield of furfural (cf. Table S1). Moreover, efficient recycling strategies need to be developed for homogeneous acid catalysts. Usually, heterogeneous catalysis is preferred for industrial application due to the ease of catalyst separation and reuse, and solid acid catalysts (e.g., zeolites, heteropoly acids, acidic resins, and functionalized metal oxides) have been extensively investigated for furanic synthesis from C5/C6 sugars.[12,13] However, poor hydrothermal stability, long reaction time (>1 h) and limited furfural yields (<80%) are still issues to be addressed (cf. Table S1).[14] Meanwhile, a frequent solid catalyst regeneration is required due to possible humin deposition on the active sites.[12,14] Thus, an efficient homogeneous catalytic process is still attractive for the scaled-up furfural production. The main demerit of homogeneous catalysis is the difficulty of downstream separation between products and catalyst. Our previous work on 5-hydroxylmethylfurfural (HMF) synthesis from glucose has demonstrated recycling of aqueous phase containing $AlCl_3$/HCl catalyst after the extractive separation of HMF.[15] This strategy should also hold for furfural synthesis, where recycling of aqueous catalyst stream can be further facilitated by tuning the reaction to reach a complete xylose conversion with a minimal humin formation and large furfural partition into the organic phase with a high extraction capacity.

Batch reactors often suffer from a poor control over flow pattern, heat/mass transfer when scaled up, which tends to limit the xylose conversion efficiency in the aqueous phase and furfural extraction to the organic phase leading to low furfural yields. Recently, microreactors have been used as a promising tool for kinetic study and production platform for HMF synthesis from C_6 sugars in monophasic or biphasic solvent systems,[15–20] due to advantages such as the superior heat/mass-transfer efficiency, precise process control, continuous operation mode, the ease of production capacity increase, and thus holding great promises for improving process sustainability and circularity.[21,22] Comparatively, few reports have been published on its application for furfural synthesis. One recent work is from Papaioannou et al.[23] who demonstrated xylose conversion to furfural over the H_2SO_4 catalyst in water-toluene biphasic systems in a slug flow millireactor (inner diameter: 4.1 mm). The furfural extraction aided by the strong inner circulation within aqueous droplets and organic slugs is claimed to greatly prevent furfural degradation. However, the furfural degradation and extraction rates were estimated to be still comparable, showing possibly mass transfer limitation that has limited the furfural yield therein (ca. up to 56%). Moreover, a better extraction solvent other than the toxic toluene could be used to increase the process sustainability.

In addition to furfural degradation, xylose-involved condensation to humins is another cause for the carbon loss in reaction. Different acids are reported to have different catalytic effects on xylose dehydration and among others, HCl gives the highest furfural yield (Table S1).[9,24] This suggests an anion effect on the reaction mechanism,[25] opening another strategy to enhance the furfural yield, that is, by reducing xylose condensation via the addition of excess beneficial anions such as chloride ions. Fulmer et al.[26] reported that NaCl promoted the activity of the acid, and the furfural yield is related to the pH of HCl/NaCl solution. Marcotullio et al.[24] studied the kinetics of xylose dehydration to furfural with different chloride salts in dilute HCl solutions and observed that Cl^- promoted the xylose conversion and furfural selectivity. Furthermore, they found that the halide anions increase the xylose dehydration rate in the order of $Cl^- > Br^- > I^-$ (which is related to the electronegativity and ion sizes) and promote the furfural selectivity in the order of $I^- > Br^- > Cl^-$ (which is related to their nucleophilicity in the aqueous solution).[25] However, in their work the effect of anions is mingled with the increased acidity and as such is not accurately captured by their kinetic model. Li et al.[27] observed a similar promoting effect of NaCl on the xylose conversion and furfural yield, as well as the humin formation in the late stage of reaction. Besides its impact on the reaction chemistry, NaCl is widely used to enhance the extraction capacity of the biphasic system via the salting-out effect (i.e., water molecule attracted by salt ions leading to a reduced solubility of a certain compound).[28] So far, though the kinetics of xylose dehydration in water has been extensively studied over the homogeneous acid catalysts (cf. a detailed overview in Table S2), a more comprehensive kinetic model including the beneficial effect of Cl^- on the xylose conversion and furfural partition in the biphasic system has not been developed yet. Such model is of great importance as it offers mechanistic insights into the Cl^--regulated xylose conversion, and new possibilities for designing reactor configurations and optimizing process parameters towards the maximized furfural yield.

Thus, to achieve an efficient furfural synthesis from xylose in high (space time) yields, this work attempted to inhibit the furfural degradation by applying water-organic biphasic systems in slug flow capillary microreactors, and to alleviate the xylose condensation by using NaCl as a promotor to improve the reaction chemistry. Reactions were firstly performed in the monophasic water system in microreactors under laminar flow at varying conditions (temperature, concentrations of substrate, HCl, and NaCl) to study the kinetics and especially the effect of NaCl on the reaction chemistry. Then, biphasic experiments were performed with methyl isobutyl ketone (MIBK) as the organic extracting phase, given that it is inexpensive, with low toxicity and high furfural partition capacity, for example, when compared with other widely used solvents such as toluene.[29] The results of biphasic experiments are well described by the kinetic model developed in monophasic experiments with incorporation of furfural extraction between phases. This shows that reaction in biphasic systems was operated under the kinetic regime, as further supported by slug flow mass transfer analysis and reaction tests at different microreactor lengths. Process optimization on the furfural yield was conducted based on the model implication. The good recyclability and reusability of the catalytic aqueous phase containing HCl/NaCl were also demonstrated. Finally, the reaction performance in this work was

compared with literature results to highlight the potential of the present process and microreactor system for an efficient furfural synthesis.

2 | EXPERIMENTAL

2.1 | Materials

D-Xylose (99 wt%), furfural (99 wt%), hydrochloric acid (37 wt%), sulfuric acid (95 wt%), and sodium chloride (99 wt%) were all purchased from Sigma-Aldrich Co., Ltd. MIBK (99 wt%) was purchased from Acros Organics Co., Ltd. All chemicals were of chemical grade and used as received without any further treatment. Mili-Q water was used to prepare solutions throughout all experiments. Perfluoroalkoxy alkane (PFA) tubings with an inner diameter (d_C) of 1.65 mm were ordered from Swagelok company and used as capillary microreactors.

2.2 | Experimental setup and procedure

Experiments on the xylose conversion catalyzed by HCl (with NaCl addition) were performed in the microreactor in both monophasic water and biphasic water-MIBK systems. Monophasic experiments were conducted firstly to study the effect of NaCl on the reaction and develop the kinetic model thereof, under a wide range of conditions corresponding to a temperature range from 120 to 180 °C, an initial concentration of the substrate (xylose or furfural) from 0.1 to 0.5 M, a concentration of HCl from 0.02 to 0.5 M, and NaCl addition between 0 and 15 wt% (cf. Table S2). Biphasic experiments were performed under a selection of the above conditions, with an inlet organic to aqueous volumetric flow rate ratio (O/A) ranging from 1 to 4.

Figure 1A displays the schematic diagram of the capillary microreactor setup for biphasic experiments, which is similar to our previous work for HMF synthesis from C6 sugars in microreactors.[15–17] The aqueous feed contained xylose, HCl, and NaCl, and the organic feed was MIBK. Both phases were delivered using a binary high-performance liquid chromatography (HPLC) pump unit (Agilent 1200 Series) at a certain O/A ratio and mixed in a polyether ether ketone Y-connector (bore diameter: 1.65 mm) in order to generate a uniform slug flow (Figure 1B) in the downstream PFA capillary microreactor. The use of the hydrophobic PFA capillary as the microreactor rendered MIBK phase as the continuous slug and the aqueous phase as discrete droplets, so that humins formed were not in direct contact with the microreactor wall, thus avoiding its deposition on the wall that could possibly lead to channel blockage.[15] The main part of the capillary microreactor was coiled around an aluminum block and placed in an oven which was set at a certain temperature (i.e., the reaction temperature). A short outlet section of the microreactor (ca. 30 cm long) outside the oven was immersed in a water bath (at ca. 20°C) in order to quench the reaction. A back pressure regulator was installed at the microreactor exit to maintain a constant pressure of ca. 10 bar to keep the reactor content in the liquid state. Product samples were collected after the system reached the steady state (i.e., after approximately 4 times the residence time in the microreactor). The length of the microreactor (L_C; i.e., the section inside the oven) is 3.3 m, except in some additional experiments to study whether there are mass-transfer limitations where microreactors of 1.2 and 16.9 m length were also used. The residence time (τ) in the microreactor was varied by adjusting the flow rates (calculation details about the actual phasic flow rate and τ are given in Section S4 of the Supporting Information). Note that the reaction occurrence in the short sections of microreactor inlet (i.e., between the Y-connector and oven) and outlet is negligible, by further considering the very low-temperature levels therein (i.e., ca. 20°C at the inlet and the fast quenching of reaction mixture to ca. 20°C at the outlet). The collected aqueous and organic products were filtered by a polytetrafluoroethylene (0.45 μm) filter, and then analyzed by HPLC and gas chromatography (GC), respectively.

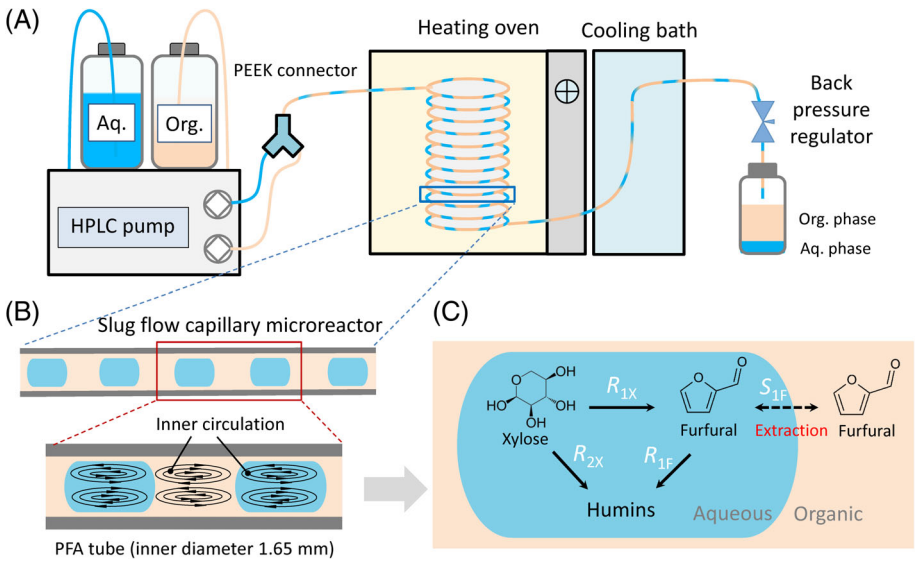

FIGURE 1 Slug flow capillary microreactor system for furfural synthesis from xylose: (A) scheme of the experimental setup; (B) slug flow pattern, where inner circulation promoted mixing/reaction in aqueous droplets and enhanced furfural extraction to organic slugs; (C) reaction network in water-MIBK systems, where reaction labels are explained in Section 3.3. HPLC, high-performance liquid chromatography; PEEK, polyether ether ketone; PFA, perfluoroalkoxy alkane

Monophasic experiments were performed in the same setup as shown above, except the organic phase flow being stopped. Before each run, the microreactor was flushed with water in order to make sure that any humins (if remained from the previous run) were removed.

The above monophasic and biphasic experiments under representative conditions were conducted at least twice, the results of which are reproducible within 5% standard deviation.

In addition, partition coefficients of furfural between water and MIBK at various temperatures and NaCl loadings, as required in the modeling of biphasic systems, were also determined (see Figure S4 and the other details in Section S5 of the Supporting Information).

2.3 | Analyses and characterization

The composition of the aqueous phase (i.e., the feed and collected product) was analyzed by an Agilent 1200 HPLC, equipped with an Agilent 1200 pump, a Waters 410 refractive index detector, a standard ultraviolet detector, and a Bio-Rad organic acid column (Aminex HPX-87H). A diluted aqueous sulfuric acid solution (5 mM) flowing at 0.55 ml min^{-1} was used as the effluent. The column temperature was at 60°C. The organic phase sample was analyzed by a TraceGC ultra GC equipped with a flame ionization detector and a Stabilwax-DA fused silica column. The component concentrations in the aqueous and organic samples were quantified from calibration curves obtained by measuring standard solutions with known concentrations.

2.4 | Definitions and calculations

The conversion of substrate "s" and the yield of product "p" are defined by

$$X_s = \frac{Q_{aq,0}C_{aq,s,0} - Q_{aq,1}C_{aq,s,1}}{Q_{aq,0}C_{aq,s,0}} \times 100\%, \quad (1)$$

$$Y_p = \frac{Q_{org,1}C_{org,p,1} + Q_{aq,1}C_{aq,p,1}}{Q_{aq,0}C_{aq,s,0}} \times 100\%, \quad (2)$$

where Q_{aq} and Q_{org} denote the volumetric flow rates of the aqueous and organic phases, respectively. C_{aq} and C_{org} represent the concentrations in the aqueous and organic phases, respectively. The subscripts 0 and 1 refer to the microreactor inlet and outlet (both at ca. 20°C), respectively. Due to the partial miscibility between MIBK and water, the outlet flow rates of the two phases slightly differ from the inlet flow rates and were corrected as

$$Q_{aq,1} = Q_{aq,0}\gamma_{aq}, \quad (3)$$

$$Q_{org,1} = Q_{org,0}\gamma_{org}, \quad (4)$$

where γ_{aq} or γ_{org} represents the ratio of the flow rates at the microreactor outlet and inlet for either the aqueous or organic phase. The values of γ_{aq} and γ_{org} were estimated by Aspen Plus simulation and provided in Table S7 (see details in Section S6 of the Supporting Information).

The carbon balance is defined by

$$\text{C balance} = \frac{\text{C amount in the products} + \text{C amount in the remaining substrate}}{\text{C amount in the starting substrate}} \times 100\%, \quad (5)$$

which is based on the quantifiable products by HPLC and GC (e.g., xylose and furfural). It does not account for the nonidentified soluble/insoluble byproducts.

3 | RESULTS AND DISCUSSION

3.1 | Monophasic experiments: Effect of NaCl addition, acid and substrate concentrations, and temperature

Firstly, monophasic experiments in water were conducted in microreactors to study the reaction kinetics using xylose or furfural as the substrate with or without the addition of NaCl. The xylose conversion over Brønsted acid catalysts in water is known to typically include xylose dehydration to furfural, furfural degradation to humins, and xylose-involved condensation reactions leading to humins.[9] The presence of NaCl is shown to increase the xylose conversion rate and furfural selectivity.[24,27] However, as NaCl has a higher affinity for water and would thus compete with H^+ for water of hydration leading to a higher acidity[30] (e.g., the pH of 0.2 M HCl solution decreases from 0.70 to 0.12 after adding 15 wt% of NaCl), the reported promoting effect of NaCl on the xylose conversion reaction in the literature is actually interconnected with the increased acidity.[24,27] To investigate the intrinsic effect of the chloride ion, here reactions of xylose and furfural in the presence of different amounts of NaCl were performed at typically 160°C under the same pH (i.e., by fine tuning of HCl concentration), as displayed in Figure 2. The conversion of xylose only presented a slight increase with the increasing NaCl concentration (up to 15 wt% as studied in this work) (Figure 2A). This indicates that the chloride ion has a minor impact on the overall xylose conversion rate, and thus the widely reported higher xylose conversion promoted by NaCl is mainly ascribed to the increased acidity in the reaction medium. Comparatively, the promoting effect of NaCl on the furfural yield is more distinct. The maximum furfural yields as well as the carbon balance are improved by adding 5 wt% of NaCl in water, followed by a gradual, but marginal decrease upon further increasing the NaCl concentration (Figure 2B,C). At 160°C and 19.6 min, the maximum furfural yield was increased from 57.7% at 89.5% xylose conversion, to 64.1% at 92.3% xylose conversion with 5 wt% NaCl addition. In the later stage of the reaction, a faster decrease in the furfural yield and carbon balance is present with a higher NaCl loading (Figure 2B,C), indicating a more significant humin formation.

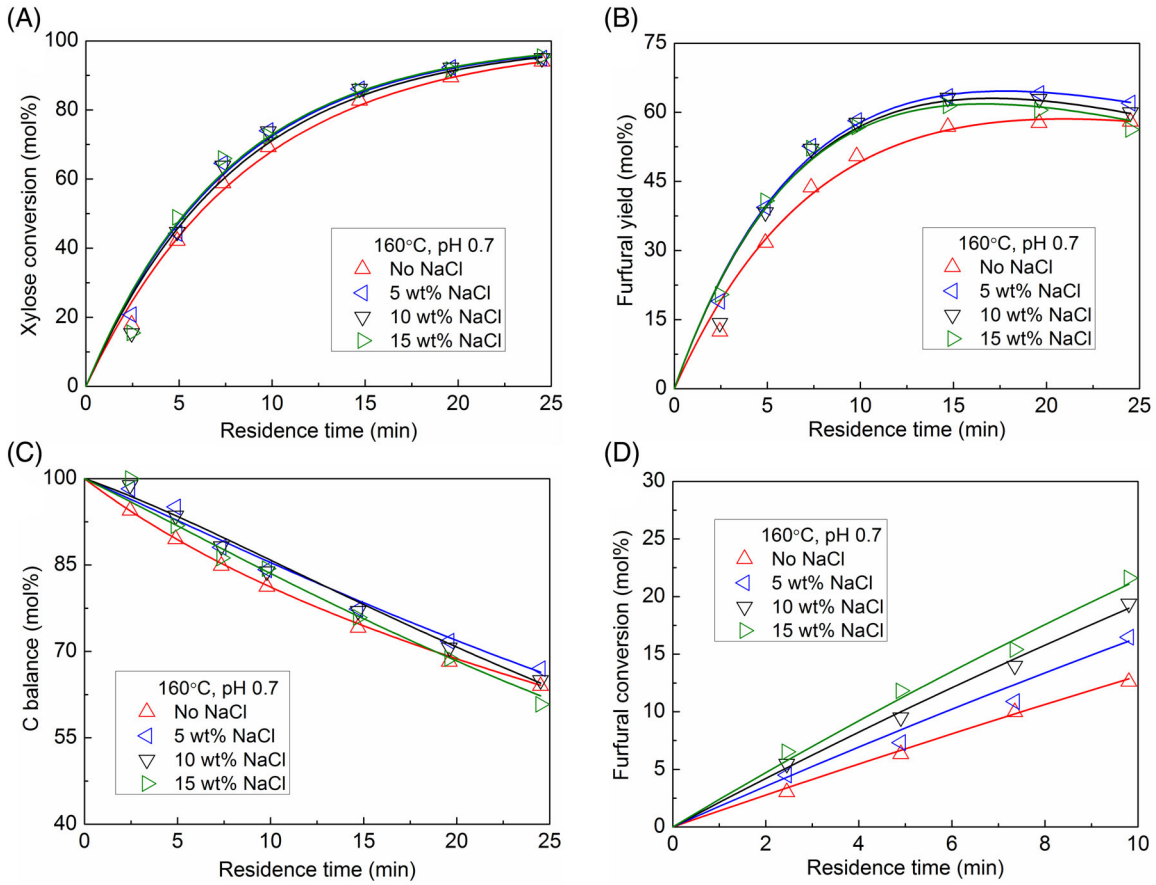

FIGURE 2 Effect of NaCl addition on (A) the xylose conversion, (B) furfural yield, (C) C balance, and (D) furfural conversion over the HCl catalyst in monophasic water in microreactors. Reaction conditions: 160°C, 0.1 M xylose (A–C) or furfural (D) as the starting substrate, pH 0.7 (at 20°C). Symbols are the experimental data and lines the model values (the same in Figures 3–5 and 8 hereafter)

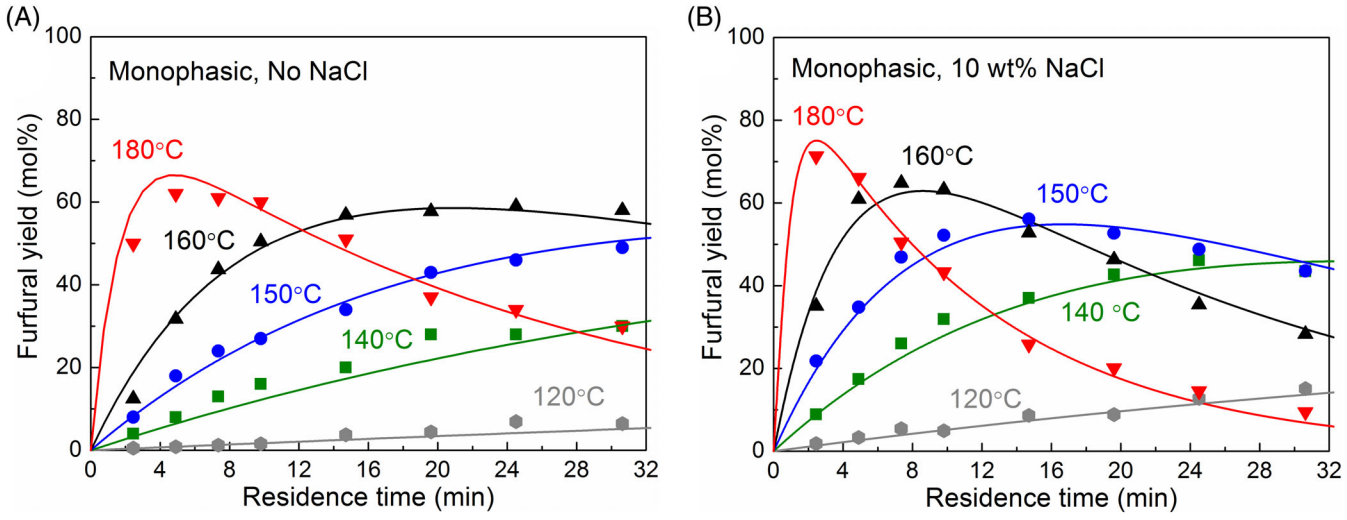

FIGURE 3 Effect of temperature on the furfural yield from xylose in monophasic water in microreactors (A) without NaCl (pH = 0.70) and (B) with 10 wt% NaCl (pH = 0.40). Reaction conditions: 0.1 M xylose, 0.2 M HCl, pH measured at ca. 20°C

The reaction starting from furfural in the presence of NaCl further suggests that chloride ions promote the furfural degradation to humins (Figure 2D). Considering that NaCl promotes both xylose dehydration to furfural (Figure 2B) and furfural degradation (Figure 2D), the xylose-involved condensation to humins must have been suppressed by NaCl to maintain an almost unchanged xylose

conversion (Figure 2A) and improve the overall carbon balance (Figure 2C) compared with the case without NaCl addition.

The acid catalyst concentration and reaction temperature are important factors determining kinetic behaviors of the xylose reaction. Generally, an increase of the acid (HCl) concentration significantly promoted the xylose conversion rate, whereas the maximum furfural yield remains similar (ca. 58%) for varying acid concentrations (Figure S6). This suggests similar reaction orders in acid among the subreactions within the xylose conversion network. Comparatively, the reaction temperature has a profound effect on both the xylose conversion (Figure S7) and furfural yield (Figure 3). An increase in temperature led to a higher xylose conversion and higher maximum furfural yield, which is even more pronounced in the presence of NaCl (Figure 3). For instance, an increase of reaction temperature from 160 to 180°C led to an increase in the maximum furfural yield from ca. 58% to 63% without NaCl, and from 62% to 72% in the presence of 10 wt% NaCl. This suggests a higher activation energy for xylose dehydration to furfural than that for furfural degradation to humins. Moreover, similar conversions of furfural and xylose (as well as the corresponding furfural yields) were observed when varying the substrate concentration (Figure S8), indicative of an overall first order with respect to the substrate. It is worth noting that beyond kinetic studies, monophasic experiments in microreactors are not the optimized operation mode, as certain amounts of solid humins were observed on the reactor wall at a prolonged residence time.

3.2 | Biphasic experiments: Effect of O/A, NaCl addition, and temperature

To promote the furfural yield and reduce the humin formation (as well as avoiding its deposition on the microreactor wall to facilitate the long-term operation), biphasic experiments were applied in microreactors under a slug flow pattern (Figure 1). The xylose conversion remains similar at different inlet organic to aqueous volumetric flow ratios (O/A; being 1, 2, or 4), and interestingly, the biphasic operation was found to give faster xylose conversion rates than monophasic reactions in microreactors (i.e., at O/A = 0), as shown in Figure S9a. Considering that MIBK is nonreactive and only serves as an extraction solvent,[15,16] such a difference in the xylose conversion is ascribed to the decreased volume of the aqueous phase due to the partial miscibility between phases at the reaction temperature (Figure S2) leading to a higher actual acid concentration that contributed to the increased xylose conversion in the biphasic operation.[16] The biphasic system also significantly improved the furfural yield. For example, an O/A ratio of 1 led to a significant increase in the maximum furfural yield from 58% (in the monophasic water system) to 72% at 160°C without NaCl, and further to 79% by further raising the O/A ratio to 4 (160°C; Figure 4A), due to a higher capacity and driving force for furfural extraction at increased O/A ratios. Besides, a limited increase in the maximum furfural yield at O/A ratios over 1 is due to the high partition coefficient of furfural in MIBK being around 7.5 at 160°C without NaCl addition (Figure S4).

The effect of NaCl addition was studied at an O/A ratio of 4 (Figure 4B). Increasing the NaCl addition leads to a higher acidity, which considerably increased the xylose conversion rates (Figure S9b). Besides, the maximum furfural yield is boosted to over 90% with NaCl addition above 10 wt% (Figure 4B). Similar to O/A, an increase of NaCl addition also enhances the driving force and capacity for furfural extraction by promoting the furfural partition into MIBK (Figure S4). However, since the furfural yield is already not much limited at O/A ratios above 1 without NaCl addition (Figure 4A) and the increased pH does not impact the maximum furfural yield (Figure S6b), NaCl should enhance the furfural yield mainly by improving the reaction chemistry of xylose conversion towards higher furfural selectivities (Figure 2).

In the biphasic system, the reaction temperature not only regulates the kinetic behavior of xylose conversion, but also affects the

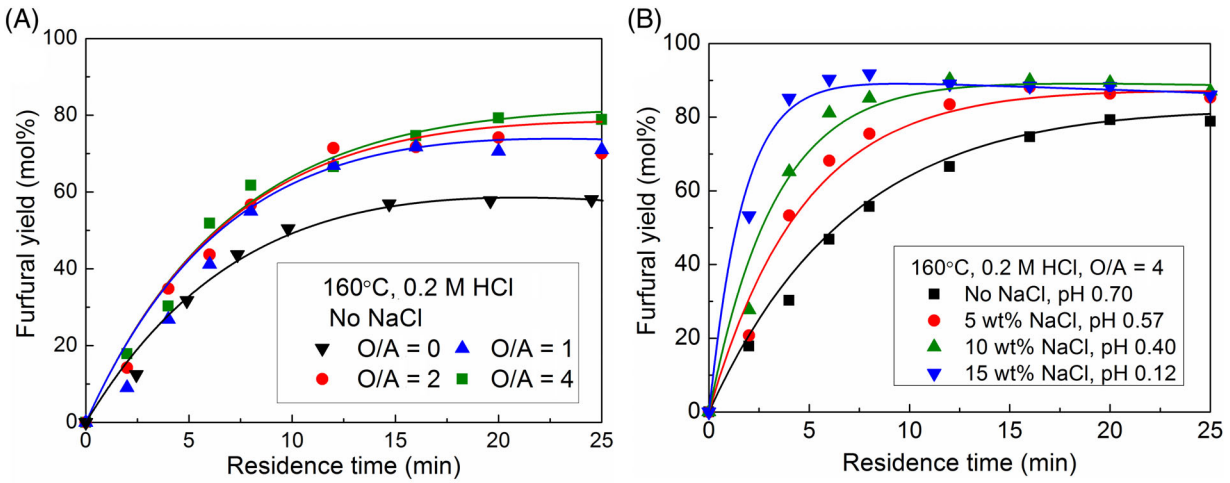

FIGURE 4 Effect of (A) the inlet organic to aqueous volumetric flow ratio (O/A) and (B) NaCl addition on the furfural yield in microreactors. Reaction conditions: 0.1 M xylose, 160°C, 0.2 M HCl, pH measured at ca. 20°C

furfural partition between the two phases. As expected, higher temperatures lead to higher xylose conversion rates (Figure S10). However, higher temperatures also result in a lower furfural partition into the organic phase (Figure S4), which is unfavorable for furfural extraction. As an integrated result, increasing the temperature still leads to a higher maximum furfural yield (Figure 5). Compared with the monophasic system (Figure 3), the difference in the maximum furfural yield between varying temperatures is less significant in this case, and furfural is more stable towards degradation due to the large partition into MIBK (Figure 5). Besides, the presence of NaCl not only promotes the xylose conversion rate (see Figure S10a,b), but also improved the overall furfural yield. For instance, the maximum furfural yield at 180°C increased from 80% at 8 min without NaCl (Figure 5A) to 93% at 4 min after adding 10% of NaCl (Figure 5B). This mainly owes to the promoted xylose dehydration and suppressed xylose condensation, as the extraction performance is not much limited by the further increased partition capacity at such an O/A (of 4) and thus the salting-out effect by NaCl addition is of less contribution.

3.3 | Kinetic modeling studies

All the current literature models regarding the xylose conversion to furfural with the presence of NaCl are not fully developed in the following aspects: (i) the effect of NaCl on the acidity via salting out is not quantified and incorporated into the model to accurately estimate the concentration of acid catalyst under the reaction conditions; (ii) the influence of NaCl on the xylose conversion chemistry (which is the most important aspect) is thus mingled with its effect on the acidity and not well addressed; (iii) correlations between the kinetic parameters and NaCl concentration were not established limiting the application of models to other reaction conditions. These are addressed in this section in order to develop a more comprehensive kinetic model.

3.3.1 | Reaction network of xylose conversion in water

The reaction network for xylose conversion in water still remains a matter of debate in the literature and diverse possibilities have been proposed so far (cf. Table S3), of which among others the three most commonly accepted mechanisms are summarized in Scheme 1. All the three reaction networks involve xylose dehydration (via intermediates) to furfural and furfural degradation to humins. The difference lies in the involvement of xylose in side reactions leading to humins, which could be by the direct xylose condensation (Scheme 1A), cross condensation between xylose and furfural (Scheme 1B) or reactions between the intermediates of xylose dehydration and furfural (Scheme 1C). In the case of a reaction between xylose and furfural (Scheme 1B), the change in the (initial) concentration of xylose or furfural in water, for example, by varying the xylose feed concentration or O/A ratio in biphasic systems, would lead to different overall xylose conversion rates.[31,32] This, however, was not observed under the prevailing conditions in this work (Figures S8 and S9), and as such this mechanism can be ruled out. In addition, the reaction between dehydration intermediates and furfural (Scheme 1C) was reported to play only a minor role compared with the direct xylose condensation (Scheme 1A),[33] and since the intermediate is not quantifiable, the relevant kinetic parameters were usually estimated based on an overall fitting.[32–34] Generally speaking, all these three reaction networks or their combinations might work well in terms of the model prediction in the monophasic water system. Nevertheless, for biphasic systems the furfural-involved cross condensation reactions should be carefully considered as they would be estimated by the model to be largely suppressed given the efficient furfural extraction, and as such lead to a deviation in the prediction of xylose conversion and furfural yield (if a direct xylose condensation is present, but excluded in the model).[31] Therefore, by further considering the ease of kinetic parameter estimation, the reaction network involving the direct xylose

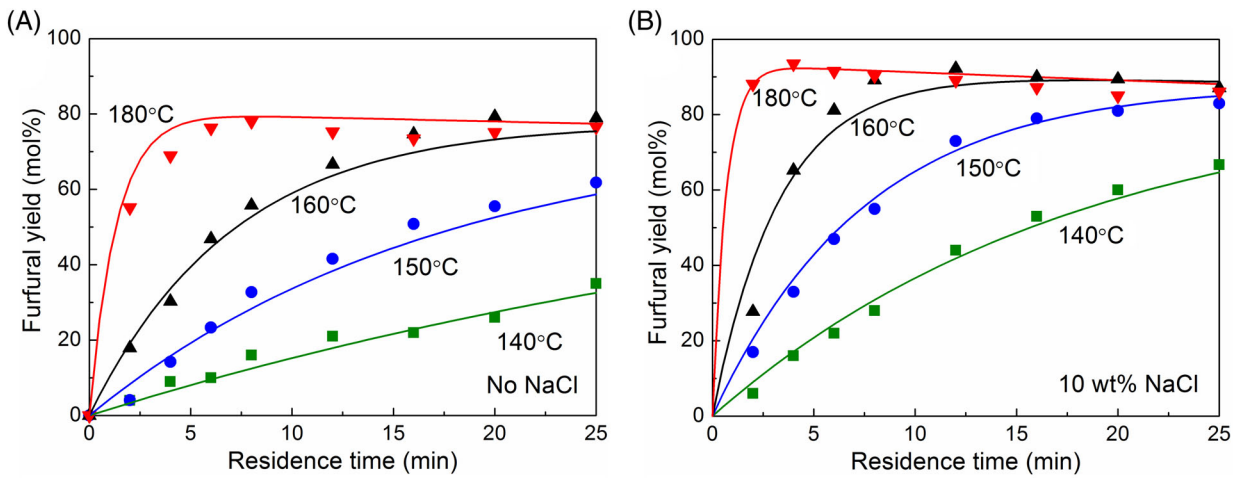

FIGURE 5 Effect of temperature on the furfural yield in slug flow microreactors (A) without NaCl and (B) with 10 wt% NaCl. Reaction conditions: 0.1 M xylose, 0.2 M HCl, O/A = 4

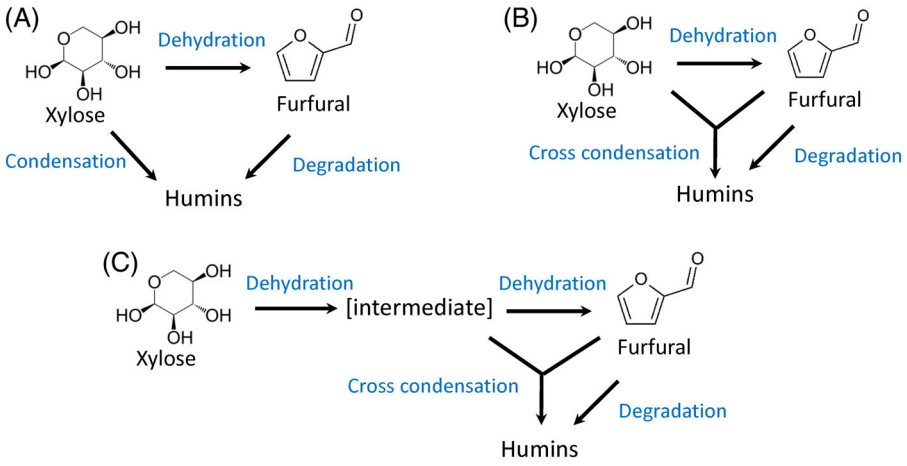

SCHEME 1 Representative reaction networks for kinetic studies of xylose dehydration over Brønsted acid catalysts in water, with different reaction pathways for humins formation from: (A) furfural degradation and xylose condensation; (B) furfural degradation and cross condensation between xylose and furfural; and (C) furfural degradation and cross condensation between the dehydration intermediates and furfural. (A) from the literature[24,32] is adopted in the current work

condensation to humins (Scheme 1A) was adapted for the current kinetic modeling for monophasic and biphasic systems, as shown in Figure 1C. The cross condensations were neglected to simplify our analysis, which does not affect the prediction of the overall humin formation from xylose and furfural.

3.3.2 | Development of the kinetic model from monophasic experiments in the microreactor

The kinetic model was developed based on the results of monophasic experiments in the microreactor with xylose or furfural as the starting substrate over a wide range of conditions (cf. Table S2). As such, dependencies of the reaction rate on parameters such as temperatures and concentrations of substrates, acid, and NaCl were all captured by the model. In monophasic microreactors, the flow pattern and the extent of axial and radial diffusion are important factors that determine the residence time distribution, and thus have been carefully considered for kinetic studies in this work (cf. details in Section S9.2 of the Supporting Information). Generally, the axial diffusion in the microreactor in such experiments is considered negligible (characterized by the sufficiently large Bodenstein numbers of xylose and furfural on the order of ca. 10^6–10^7). Moreover, the fluid is under laminar flow with a parabolic velocity profile, which however can be compensated by the fast radial diffusion (characterized by the Fourier numbers of xylose and furfural being [much] larger than 1) to afford an approximate plug flow behavior.[35] Thus, here a simplified plug flow model was adopted for kinetic modeling.

Based on the network of xylose reaction in water (Scheme 1A and Figure 1C), the mole balance of xylose and furfural is expressed as

$$\frac{dC_{\mathrm{aq,\ Xyl}}}{d\tau} = -R_{1X} - R_{2X}, \tag{6}$$

$$\frac{dC_{\mathrm{aq,\ FF}}}{d\tau} = R_{1X} - R_{1F}, \tag{7}$$

where $C_{\mathrm{aq,Xyl}}$ and $C_{\mathrm{aq,FF}}$ are the concentrations of xylose and furfural in the aqueous phase, respectively. R_{1X}, R_{2X}, and R_{1F} denote the reaction rates for xylose dehydration to furfural (xylose → furfural + $3H_2O$), xylose condensation (xylose → humins) and furfural degradation to humins (furfural → humins), respectively. The kinetic models in most literatures assume a first order in the reactant and acid catalyst (cf. Table S3).[9] In the present work, experiments on reactions from xylose and furfural at different substrate and acid concentrations have been performed (Figures S6 and S8). Figure S8 shows that the sugar conversion (and the corresponding furfural yield) and the furfural conversion are independent of substrate concentrations. Therefore, a first-order dependence on the reactant is assumed for all subreactions. In other words, a power-law approach (with reaction orders as unknown parameters) is unnecessary. Then, the individual reaction rates in Figure 1C are defined as

$$R_{1X} = k_{\mathrm{app,\ 1X}} C_{\mathrm{aq,\ Xyl}}, \tag{8}$$

$$R_{2X} = k_{\mathrm{app,\ 2X}} C_{\mathrm{aq,\ Xyl}}, \tag{9}$$

$$R_{1F} = k_{\mathrm{app,\ 1F}} C_{\mathrm{aq,\ FF}}, \tag{10}$$

where $k_{\mathrm{app},ij}$ ($i = 1$ or 2; $j =$ X or F) is the apparent kinetic constant for each subreaction.

In the current setup (Figure 1A), the heating-up stage (i.e., raising the temperature from the inlet room temperature to the oven temperature as the target reaction temperature in the microreactor) can be finished within seconds due to the excellent heat transfer efficiency of the microreactor (cf. Section S9.5),[15] and thus is neglected for kinetic modeling in this work. After heating-up, the volumetric flow rate of the aqueous phase at the reaction temperature T (Q_{aq}) differs from its initial value at ca. 20°C ($Q_{\mathrm{aq,0}}$), and is corrected as

$$Q_{\mathrm{aq}} = Q_{\mathrm{aq,0}} \alpha_{\mathrm{mono,aq}}, \tag{11}$$

where $\alpha_{\mathrm{mono,aq}}$ (ranging from 1.06 to 1.14 within 120–180°C; cf. Figure S2a) is the ratio of the densities of the aqueous phase at 20°C and T, and can be estimated as a function of T (in °C; see Section S4 of the Supporting Information for details) from

$$\alpha_{\text{mono,aq}} = 0.921 + 0.062e^{0.007T}. \quad (12)$$

To account for the phase volume change, the conversion and yield are calculated as

$$X_s = \frac{C_{\text{aq,s,0}} - \alpha_{\text{mono,aq}} C_{\text{aq,s}}}{C_{\text{aq,s,0}}} \times 100\%. \quad (13)$$

$$Y_p = \frac{\alpha_{\text{mono,aq}} C_{\text{aq,p}}}{C_{\text{aq,s,0}}} \times 100\%. \quad (14)$$

In summary, the kinetic model for the xylose conversion derived from monophasic experiments in the current microreactor comprises of a set of nonlinear ordinary differential equations for the mole balances of xylose and furfural (Equations (6) and (7)) and the reaction rates (Equations (8)–(10)), together with equations to describe the volume change (Equations (11) and (12)). Apparent kinetic parameters ($k_{\text{app},ij}$) were then determined by processing the experimental data simultaneously in Matlab R2010a (MathWorks) using the *lsqnonlin* nonlinear least-squares fitting function, based on a Trust-region-reflexive algorithm to perform a local minimization of the errors between the model values and experimental data (i.e., on the reactant conversion and product yields).

At a certain reaction temperature, the proton concentration in the aqueous phase (C_{H^+}) is a function of the concentrations of HCl (C_{HCl}) and NaCl (C_{NaCl}), and can be estimated by[30]

$$\log C_{H^+} = \log C_{\text{HCl}} - (0.18 + 0.006\Delta H_s) C_{\text{NaCl}}, \quad (15)$$

where C_{H^+}, C_{HCl}, and C_{NaCl} are all in M. Considering the phase volume change, for a given set of initial concentrations of HCl and NaCl at 20°C ($C_{\text{HCl,0}}$ and $C_{\text{NaCl,0}}$), there are $C_{\text{HCl}} = C_{\text{HCl,0}}/\alpha_{\text{mono,aq}}$ and $C_{\text{NaCl}} = C_{\text{NaCl,0}}/\alpha_{\text{mono,aq}}$ at the reaction temperature. ΔH_s is the enthalpy of NaCl solution (kcal mol^{-1}) and is estimated as a function of T (in K) empirically by[36]

$$\Delta H_s = 41.587 - 0.3159T + 8.514 \times 10^{-4}T^2 - 8.3637 \times 10^{-7}T^3. \quad (16)$$

In the case of a first-order dependency on the acid catalyst, the obtained $k_{\text{app},ij}$ in our work should be linearly dependent on C_{H^+}, which has been correctly reflected in the current experiments (cf. Figure S12). Consequently, it is reasonable to describe $k_{\text{app},ij}$ as

$$k_{\text{app},ij} = k_{ij} C_{H^+}, \quad (17)$$

where k_{ij} is the intrinsic kinetic constant (i.e., with the kinetic effect of Cl^- incorporated) for each subreaction. The best estimation of k_{ij} values and their standard deviation are given in Table 1 for the reference temperature of 160°C as a typical example. For a given amount of NaCl addition in the presence of HCl catalyst (or a given Cl^- concentration), the kinetic constant of xylose dehydration to furfural (k_{1X}) is far higher than those of side reactions leading to humins (k_{2X} and k_{1F}), indicating that furfural formation is preferred in the xylose conversion and thus high furfural yields are feasible via process optimization. At a higher NaCl concentration, the kinetic constants for xylose dehydration (k_{1X}) and furfural degradation (k_{1F}) to humins increased whereas that for xylose condensation (k_{2X}) decreased (cf. Figures S12, S14, and S16 as well), which supports that the presence of NaCl not only enhanced furfural formation and suppressed xylose condensation, but also promotes furfural degradation, corroborating the importance of a proper NaCl addition for process optimization (Figure 2). To account for the kinetic effect of Cl^-, the kinetic constants as a function of the concentration of chloride ions at the reaction temperature (C_{Cl^-}) are modeled as

$$k_{1X} = q_1 + q_2 e^{q_3 C_{Cl^-}}, \quad (18)$$

$$k_{2X} = q_4 C_{Cl^-}^{q_5}, \quad (19)$$

$$k_{1F} = q_6 + q_7 C_{Cl^-}, \quad (20)$$

where $C_{Cl^-} = C_{\text{HCl}} + C_{\text{NaCl}}$ and the fitting parameters q_1–q_7 were estimated as a function of the temperature (Equations S17–S26; cf. details in Section S9.4 in the Supporting Information). With Equations (18)–(20), for given initial concentrations of HCl and NaCl (i.e., C_{Cl^-} being up to ca. 3 M), k_{ij} values within the temperature range (120–180 °C) can be estimated and used to predict the reaction kinetics with known initial xylose concentrations.

Values of the apparent activation energy (Ea_{ij}) for each subreaction are also listed in Table 1 for a certain Cl^- concentration. It was estimated from the temperature dependency of k_{ij} according to the Arrhenius equation, that is,

$$k_{ij} = k_{ij,\text{Ref}} \exp\left[\frac{Ea_{ij}}{R}\left(\frac{T - T_{\text{Ref}}}{T T_{\text{Ref}}}\right)\right]. \quad (21)$$

Here $k_{ij,\text{Ref}}$ is the kinetic constant at the reference temperature (T_{Ref}) of 160°C. Ea_{ij} was estimated by fitting $\ln k_{ij}$ vs. $1/T$ according to Equation (21). The activation energy for xylose dehydration (Ea_{1X}) is higher than those for xylose condensation (Ea_{2X}) and furfural degradation (Ea_{1F}), suggesting the possibility of increasing the furfural yield at a higher reaction temperature, in line with the experimental observations (Figure 3) and literature models.[9] At a higher NaCl or Cl^- concentration, the estimated Ea_{1X} and Ea_{2X} increased slightly, and Ea_{1F} became lower. Among others, the increased Ea_{1X} does not contradict the kinetically favoring effect by Cl^- given the significant increase of k_{1X} herein (Table 1). In other words, a higher k_{1X} value is associated with the largely increased pre-exponential factor. Notably, a similar activation energy increase with Cl^- addition can be also observed in the work by Li et al.[37] (for xylose dehydration to furfural) and Mellmer et al.[38] (for fructose dehydration to HMF). The observed variation of Ea_{ij} with Cl^- concentration is because a simplified model was used in this work to describe the xylose conversion with NaCl addition, whereas some Cl^--involved intermediate reactions and the reaction orders thereof were not included. As such the estimated values of Ea_{ij} are still apparent and empirical, which might (slightly) deviate

TABLE 1 Kinetic parameters for the xylose conversion to furfural over the HCl catalyst with or without NaCl addition

			Kinetic constant at 160°C (L mol^{-1} min^{-1})			Activation energy (kJ mol^{-1})		
Entry	C_{NaCl}[a] (wt%)	C_{Cl^-}[b] (M)	k_{1X}	k_{2X}	k_{1F}	Ea_{1X}	Ea_{2X}	Ea_{1F}
1	0	0.180	0.498 ± 0.036	0.136 ± 0.040	0.078 ± 0.012	139.7 ± 4.4	131.9 ± 6.3	85.4 ± 5.1
2	5	0.855	0.665 ± 0.043	0.083 ± 0.004	0.105 ± 0.013	141.5 ± 5.4	134.5 ± 8.4	83.4 ± 7.0
3	10	1.585	0.756 ± 0.080	0.076 ± 0.008	0.143 ± 0.011	143.2 ± 2.2	136.6 ± 5.1	72.2 ± 7.2
4	15	2.839	0.888 ± 0.074	0.061 ± 0.006	0.202 ± 0.013	145.1 ± 2.9	137.8 ± 6.4	72.5 ± 1.3

[a]Concentration of NaCl in the aqueous phase at 20°C.
[b]Concentration of chloride ions at the reference temperature of 160°C, $C_{Cl^-} = C_{HCl} + C_{NaCl}$.

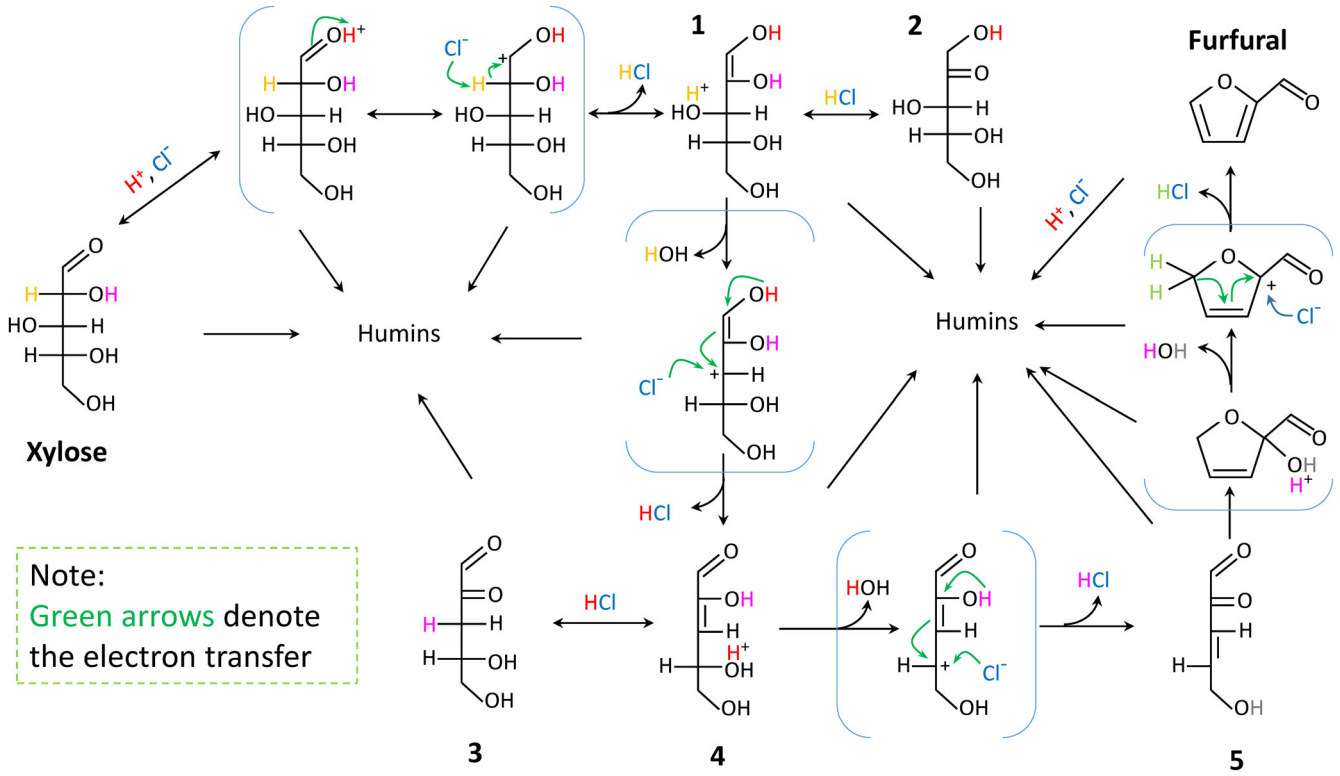

SCHEME 2 Proposed mechanism of xylose dehydration in water over the HCl catalyst (promoted by NaCl)

from those derived from the actual reaction mechanism (see Scheme 2 for the mechanism proposed in this work and Section 3.4 for more discussion).

It should be noted that the above kinetic modeling assumes an isothermal process in the microreactor, as verified in Section S9.5 of the Supporting Information given the mild reaction heat of the endothermic xylose dehydration reaction (ca. 80 kJ mol^{-1})[39] and the superior heat transfer characteristics of the microreactor.

3.3.3 | Mass transfer analysis in the biphasic slug flow microreactor

In the biphasic system under slug flow operation in microreactors, the formed furfural was transferred from aqueous droplets to organic slugs, through (i) the MIBK film between the droplet and microreactor wall and (ii) the caps of the droplet (Figure 6A). The pathway (ii) is estimated to be dominant in mass transfer given a fast film saturation (see calculation details in Section S9.6 of the Supporting Information), which leads to a simplified estimation of the overall liquid–liquid mass transfer coefficient (K_L) based on the model of Van Baten et al.[40] as

$$K_L = \frac{1}{\frac{1}{\frac{2\sqrt{2}}{\pi}\sqrt{\frac{D_{aq,FF}U_{slug}}{d_c}}} + \frac{1}{m\frac{2\sqrt{2}}{\pi}\sqrt{\frac{D_{org,FF}U_{slug}}{d_c}}}}, \quad (22)$$

where $D_{aq,FF}$ and $D_{org,FF}$ are the diffusivities of furfural in the aqueous and organic phases, respectively (Table S8). U_{slug} is the slug velocity (i.e., two-phase mixture velocity $\overline{u}$, as calculated by Equation (S4)). The

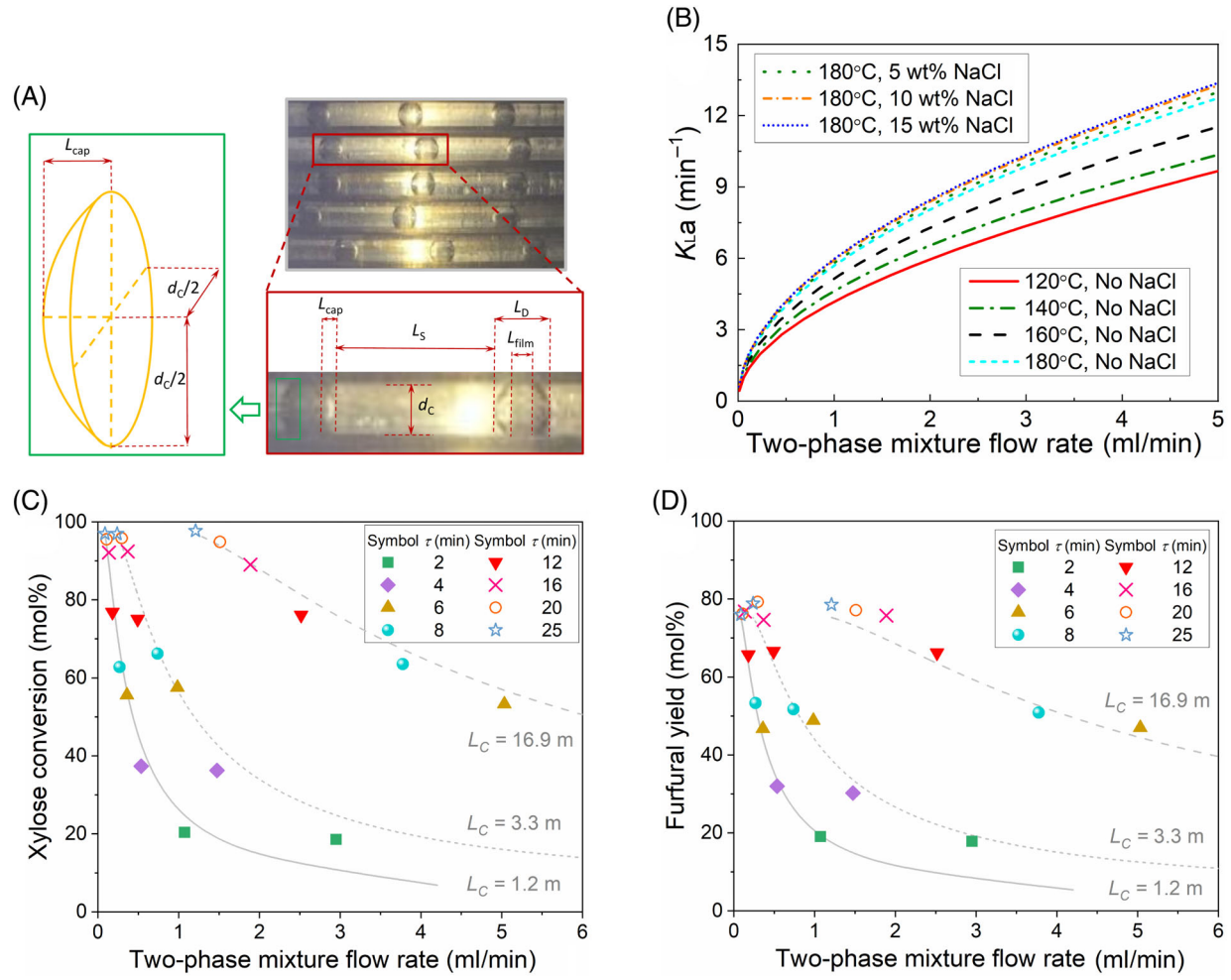

FIGURE 6 (A) Image of the slug flow in the present perfluoroalkoxy alkane (PFA) microreactor and the simplified schematics of the cap geometry of the aqueous droplet; (B) the estimated overall liquid–liquid volumetric mass transfer coefficients as a function of the two-phase mixture flow rate (O/A = 4); (C) xylose conversion and (D) furfural yield vs. the two-phase mixture flow rate in the slug flow microreactor of different lengths (L_C = 1.2, 3.3, or 16.9 m; τ is the residence time). Reaction conditions: 160°C, 0.1 M xylose, 0.2 M HCl, O/A = 4

specific interfacial area of the cap region was calculated based on the lengths of the droplet, slug, and cap (denoted as L_D, L_S, and L_{cap}, respectively) measured from the slug flow image shown in Figure 6A. The cap is assumed to be of the oblate spheroid shape with three elliptic radii approximated as $d_C/2$, $d_C/2$, and L_{cap}. Thus, there is[41]

$$a_{cap} = \frac{\frac{\pi}{2} d_C^2 + \pi \frac{L_{cap}^2}{e} \ln\left(\frac{1+e}{1-e}\right)}{\frac{\pi}{4} d_C^2 (L_D + L_S)}, \quad (23)$$

where e is the ellipticity of the oblate spheroid and defined as

$$e = \sqrt{\left(\frac{d_C^2}{4}\right) - L_{cap}^2} \Big/ \frac{d_C}{2}. \quad (24)$$

The estimated values of K_La (at an inlet O/A ratio of 4) for different temperatures and NaCl additions are presented in Figure 6B. Apparently, higher flow rates (or equivalently, higher droplet/slug velocities) lead to higher mass transfer coefficients as a result of the enhanced inner circulation in the droplets and slugs.[42] A temperature increase leads to a higher K_La, primarily due to higher diffusivities of furfural in water and MIBK (Table S8). Besides, the addition of NaCl raises K_La by increasing the partition coefficient, though to a slight extent.

In the presence of mass transfer limitation, higher furfural yields are expected in longer microreactors at the same residence time. Hence, the xylose dehydration reactions in the biphasic system were further performed in slug flow microreactors of different lengths (1.2, 3.3, and 16.9 m) to infer the mass transfer influence, where different flow rates were applied to maintain the same residence time. As displayed in Figure 6, generally no significant difference in the xylose conversion and furfural yield was found between different microreactor lengths (Figure 6C,D), indicating the absence of mass transfer limitation in the current system. This is in line with the fact that the estimated values of K_La under our experimental conditions

(being 1.5–5.4 min^{-1} for $L_C = 1.2$ m, 2.5–8.9 min^{-1} for $L_C = 3.3$ m, and 5.6–10.0 min^{-1} for $L_C = 16.9$ m) which appear to be one or two orders of magnitude greater than the apparent rate constants of furfural formation ($k_{app,1X}$; being 0.108 min^{-1}) and degradation ($k_{app,1F}$; being 0.0172 min^{-1}) at 160°C with 0.2 M HCl, indicating that the produced furfural could be instantly extracted to MIBK before its degradation. Consequently, both the simplified mass transfer calculation and experimental results indicate that the mass transfer resistance was (largely) eliminated and the reaction was performed (predominantly) in the kinetic regime with an immediate equilibrium extraction of furfural between the aqueous and organic phases.

3.3.4 | Kinetic modeling of xylose conversion in the biphasic system in the microreactor

In the biphasic system, the volumetric flow rates of both phases changed after mixing and heating from 20°C to the reaction temperature (T) in the microreactor due to the partial miscibility between phases and liquid density change. Therefore, the actual flow rates of two phases are corrected as

$$Q_{aq} = Q_{aq,\,0}\alpha_{bi,\,aq}, \tag{25}$$

$$Q_{org} = Q_{org,\,0}\alpha_{bi,\,org}, \tag{26}$$

where $\alpha_{bi,aq}$ or $\alpha_{bi,org}$ is the correction factor denoting the ratio of the actual flow rate after mixing at reaction temperature (T) to the initial flow rate at 20°C for either the aqueous or organic phase. For a given inlet O/A ratio at 20°C and a certain NaCl addition, α is approximated as

$$\alpha = u + ve^{wT}, \tag{27}$$

where T is in °C and the values of u, v, and w are given in Table S4 for the aqueous and organic phases separately (see Section S4 of the Supporting Information for details).

It is known that the slug flow gives a narrowed residence time distribution close to that of plug flow,[43] and thus a plug flow behavior was assumed for kinetic modeling here. Then, the concentrations of furfural in both phases (i.e., $C_{aq,FF}$ and $C_{org,FF}$) are described by

$$\frac{dC_{aq,FF}}{d\tau} = R_{1X} - R_{1F} - S_{1F}, \tag{28}$$

$$\frac{dC_{org,FF}}{d\tau} = \frac{Q_{aq}}{Q_{org}}S_{1F}, \tag{29}$$

where S_{1F} represents the extraction rate of furfural from the aqueous phase to the organic phase (Figure 1C) and is calculated as

$$S_{1F} = K_L a\left(C_{aq,FF} - \frac{C_{org,FF}}{m}\right). \tag{30}$$

In biphasic experiments, since the mass transfer limitation has been both theoretically estimated and experimentally proven to be absent (cf. Section 3.3.3), the furfural concentrations in both phases were assumed to reach equilibrium immediately, as expressed by

$$C_{org,FF} = mC_{aq,FF}. \tag{31}$$

Here m is the partition coefficient of furfural between the two phases at the involved reaction temperature. In this work, m values at different temperatures and NaCl additions were measured and are approximated as (Figure S4; see Section S5 in the Supporting Information)

$$m = a - bT, \tag{32}$$

where the values of coefficients a and b with different NaCl additions are given in Table S6.

By combining with Equations (29) and (31), Equation (28) is further simplified to

$$\frac{dC_{aq,FF}}{d\tau} = \frac{R_{1X} - R_{1F}}{1 + m\frac{Q_{org}}{Q_{aq}}}. \tag{33}$$

For given concentrations of HCl and NaCl at 20°C (i.e., $C_{HCl,0}$ and $C_{NaCl,0}$), the concentrations of HCl and NaCl at the reaction temperature needed for the estimation of C_{H^+} (with Equation (15)) and kinetic constants (with Equations (19)–(21)) are corrected as $C_{HCl} = C_{HCl,0}/\alpha_{bi,aq}$ and $C_{NaCl} = C_{NaCl,0}/\alpha_{bi,aq}$, respectively. The initial substrate concentration used for kinetic modeling is also corrected as $C'_{aq,s,0} = C_{aq,s,0}/\alpha_{bi,aq}$. Then, the biphasic system modeling was performed by solving the differential equation (Equation (33)) in Matlab based on the estimated kinetic constants (Table 1 and Equations (19)–(21)), subject to additional conditions including Equations (25)–(27) (for the phasic flow rate change) and Equations (31) and (32) (for the furfural concentration in the organic phase). With the modeled component concentration during the reaction, the substrate conversion and product yield in the biphasic system in the microreactor are predicted by

$$X_s = \frac{C_{aq,s,0} - \alpha_{bi,aq}C_{aq,s}}{C_{aq,s,0}} \times 100\%. \tag{34}$$

$$Y_p = \frac{Q_{org}C_{org,p} + Q_{aq}C_{aq,p}}{Q_{aq,0}C_{aq,s,0}} \times 100\%. \tag{35}$$

3.3.5 | Evaluation of kinetic model for monophasic and biphasic systems

The performance of the developed kinetic model was evaluated by comparing its prediction with the experimental data using parity plots for both monophasic and biphasic systems (Figure 7A,B), and the representative kinetic profiles (Figures 2–5, Figures S6, S7, S9, S10). The

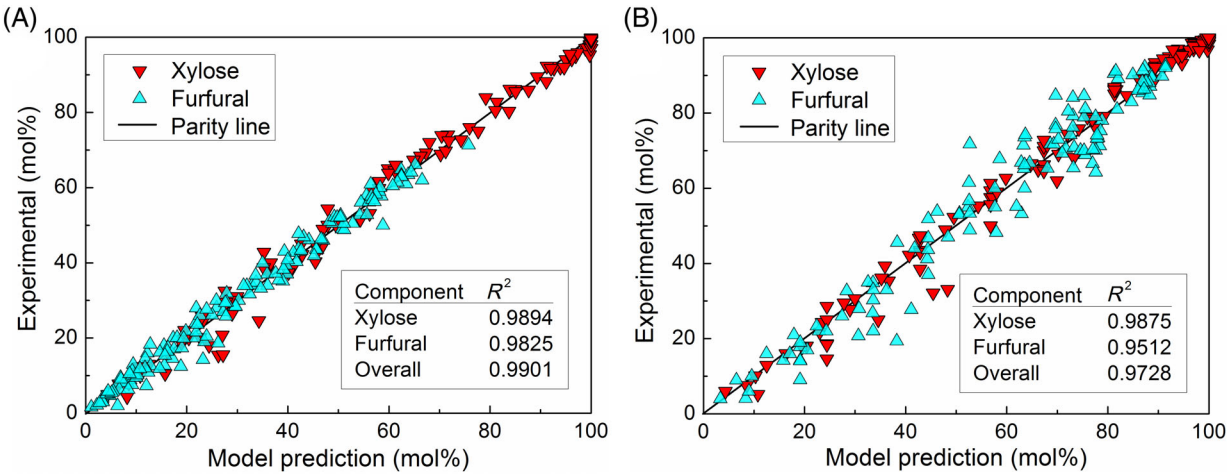

FIGURE 7 Parity plot for the model values and experimental results for the xylose conversion and furfural yield in the (A) monophasic system and (B) biphasic system in the microreactor

goodness of fit was assessed by the coefficient of determination (R^2) calculated by

$$R^2 = 1 - \sum_{i=1}^{n} (x_i - \hat{x}_i)^2 / \sum_{i=1}^{n} (x_i - \bar{x}_i)^2, \quad (36)$$

where x_i is the experimental data of xylose or furfural and $\hat{x}_i$ is the predicted model value. $\bar{x}_i$ and n represent the average and number of the experimental data, respectively.

For the monophasic system, the developed kinetic model precisely predicts the evolution trend of xylose and furfural during the reaction (Figure 2, Figures S6 and S7), and a good fit was obtained between the model predictions and experimental data with the overall R^2 close to 1 ($R^2 = 0.9901$; Figure 7A). After the incorporation of the furfural extraction step, this model was extended to predict the reaction in the biphasic system. Though the biphasic results were not used for kinetic parameter estimation, a satisfactory model prediction accuracy was achieved (cf. Figure 4, Figures S9 and S10) with the overall R^2 being 0.9728 (Figure 7B), further supporting the validity of the developed kinetic model.

Subsequently, the current experimental results were compared with the literature model predictions. Given the scarcity of the existing models incorporating the effect of NaCl on the xylose conversion, we compared only the representative experimental results without NaCl addition in this work to the predictions from some typical literature models (using HCl, H_2SO_4, or formic acid as the catalyst).[24,31–33] A detailed discussion is provided in Section S10 of the Supporting Information. Generally, for reactions in the monophasic water system, models of Marcotullio et al.,[24] Weingarten et al.,[31] and Krzelj et al.[32] with mineral acid catalysts (HCl or H_2SO_4) largely underestimate the reaction rate (i.e., both the xylose consumption and furfural formation rates) in microreactors, though they can capture more or less satisfactorily the measured furfural yield/selectivity as a function of the xylose conversion (Figure S19a–c). This implies that additional effects (e.g., nonnegligible heating-up stage in the conventional batch reactors) contributing to a relatively low reaction rate might not be fully considered when developing these models. A significant overestimation in both the reaction rate and furfural selectivity was noticed in the model of Lamminpää et al.[33] using highly concentrated formic acid (ca. up to 30 wt%) as the catalyst, possibly due to the changed reaction environment (relatively low water content and solvation effects). The above literature models were further combined with the furfural extraction step to predict reaction results in the current water-MIBK biphasic system in microreactors. A similar underestimation of the reaction rate in the model prediction is present (Figure S20a,b). Given the efficient extraction by slug flow microreactors suppressing all furfural-involved side reactions, a very high and unpractical furfural selectivity close to 100% was predicted by models of Weingarten et al.[31] and Krzelj et al.[29] that do not include the direct xylose condensation in the reaction network (Figure S20c). This indicates that at least the direct xylose condensation should not be ignored, which further demonstrates the rationality of the reaction network adapted in our model (Scheme 1A) that gives a reasonable and good prediction for both monophasic and biphasic experiments.

The activation energies estimated for the subreactions of xylose conversion in this study and the literature using various homogeneous catalysts (without addition of NaCl) were summarized and compared (cf. Table S3 and Figure S21, and a detailed discussion in Sections S3 and S11 in the Supporting Information). Generally, the estimated activation energies for xylose dehydration, furfural degradation, and xylose condensation in this work are in a similar value range to the literature ones, further supporting the validity of the current model. Some differences in the activation energies for furfural degradation and xylose condensation were found between models using different acid catalysts, which could be due to the anion effect (Figure S21b,c). A difference in activation energies for furfural degradation was also found between models using different reaction networks (Figure S21c).

3.4 | Mechanistic insights into the Cl^--promoted xylose dehydration to furfural

Chloride ions have been reported to promote the dissolution of saccharides such as cellulose via the Cl···H—O hydrogen bonding.[44,45] A similar interaction between chloride ions and hydroxyl groups of xylose is believed conducive to the formation of reaction intermediates and thus to regulating the xylose reaction.[25] So far, mechanisms of xylose dehydration to furfural still remain controversial due to technical difficulties to follow all the reaction intermediates.[9] The most accepted mechanism suggests that xylose dehydration proceeds via an acyclic form through a 1, 2-enediol intermediate and three dehydration steps to yield furfural.[9,24] Based on the results in the literature[24,25] and this work, a mechanism of xylose dehydration promoted by NaCl in water is proposed (Scheme 2). In this mechanism, side reactions from the dehydration intermediates, in addition to xylose and furfural, are also assumed. Such mechanism can still be described by the reaction network in Figure 1C, considering R_{2X} as the sum of all the possible side reactions involving xylose and its dehydration intermediates. In the proposed mechanism, due to the strong electronegativity, Cl^- ions act as weak conjugate bases assisting the enolization reaction via the proton transfer between C-2 and C-1, and promote the formation of the 1,2-enediol **1** from the protonated acyclic xylose, which is the rate-limiting step for xylose dehydration (R_{1X}).[24] This is reflected in the increased k_{1X} at higher Cl^- concentrations (Table 1 and Figure S12). After the enolization step, the 1,2-enediol **1** undergoes the first and second dehydration steps at C-3 and C-4 to form **4** and **5**, respectively, followed by the final ring closure and intramolecular dehydration to yield furfural. The enediol **1** and **4** could also transform reversibly to their ketose isomers **2** and **3**, respectively. The improved furfural selectivity at higher Cl^- concentrations is attributed to not only the enhanced xylose dehydration (i.e., increased k_{1X}), but also the suppressed xylose condensation (i.e., decreased k_{2X}) (Table 1 and Figure S14). As such, it is proposed that Cl^- ions promote the three dehydration steps by stabilizing the carbenium transition states leading to **4**, **5** and furfural, and thus reduce side reactions involving these intermediates.[25] In addition, it is found that adding Cl^- promotes furfural degradation (i.e., increased k_{1F}) (Table 1 and Figure S16). Furfural degradation involves a series of addition, substitution, condensation, and ring cleavage reactions, and all these reactions occur among the by-products leading to a polymeric network structure (humins).[46] So far, furfural degradation mechanism has not been extensively studied, and Cl^- ions are believed to interact with the degradation intermediates and promote the corresponding side reactions (still under our investigation).

3.5 | Process optimization in microreactors and catalyst recyclability

The developed kinetic model can reveal fine details in monophasic and biphasic experiments in microreactors for further process understanding and optimization. The modeled xylose conversion in monophasic water systems in the microreactor at 120–180°C without NaCl addition shows the increased humin formation from both xylose condensation and furfural degradation during the reaction, eventually leading to a sharp decrease in the furfural yield from the maxima (Figure S22a,b). Higher temperatures promote the maximum furfural yield by suppressing humin formation (particularly from furfural degradation as the major cause for carbon loss at 100% xylose conversion). Thus, switching to the biphasic operation is important to improve the furfural yield. The modeling for biphasic water-MIBK systems in microreactors (O/A = 4) proves the large suppression of the yield of humins from furfural degradation, which significantly boosts the maximum furfural yield compared with monophasic systems (e.g., from 66% to 80% at 180°C without NaCl addition; Figure S22b,d). The model also correctly addresses the beneficial effect of NaCl addition by suppressing xylose condensation (due to the kinetic effect of Cl^-) and furfural degradation (due to the enhanced extraction capacity of organic phase), as shown at 180°C and O/A = 4 (Figure S22e,f). As a result, the maximum furfural yield is boosted from 80% to 92.5% by adding 10 wt% NaCl (in line with the experimental results in Figure 4B). Besides, increasing NaCl addition from 10 to 15 wt% leads to little further increase in the furfural yield. The high furfural yield obtained in the current biphasic system is further supported by the mass transfer sensitivity analysis on furfural yields (cf. Figures S23–S25): (i) a sufficiently high k_La (ca. >3 min^{-1}) readily realized in slug flow microreactors (Figure 6B); (ii) a high m readily obtained by adding NaCl (e.g., m = 12 with 10 wt% NaCl at 180°C; Figure S4); and (iii) a moderate O/A of 4 to balance the interfacial area, driving force and capacity for furfural extraction, and the applicability issues (e.g., costs for downstream separation and recycling). Thus, an equilibrium furfural extraction could be well assumed in the model. Detailed discussion on the above model implications is provided in Section S12 of the Supporting Information. Notably, since the reaction running under the kinetic regime has been proven both theoretically and experimentally (cf. Section 3.3.3), the effect or optimization of slug size on the reaction performance is only related to that of O/A. As such, studies on other factors (e.g., the microreactor diameter, inlet mixer geometry, and the total flow rates) that affect slug sizes are beyond the scope of this work.

Based on the above experimental results and model implications, favorable process conditions such as 180°C, 10 wt% NaCl, and O/A = 4 were adapted in combination with 0.2 M HCl and a higher xylose concentration (i.e., 1 M; instead of 0.1–0.5 M in the previous experiments as shown in Table S2) to further optimize furfural synthesis in microreactors. A highest furfural yield of 93% was obtained within a short residence time of 4 min at a complete xylose conversion, also well in agreement with the model prediction (Figure 8A). Despite the higher xylose concentration in use, the confinement of reaction in the dispersed aqueous droplets prevented deposition of humins (still formed in little amount) on the microreactor wall, which ensured a steady continuous operation. The good catalyst recyclability was also demonstrated in these optimization experiments at the optimized residence time of 4 min (Figure 8B). Since the majority of furfural (over 98%; i.e., at the product collection temperature of 20°C) was

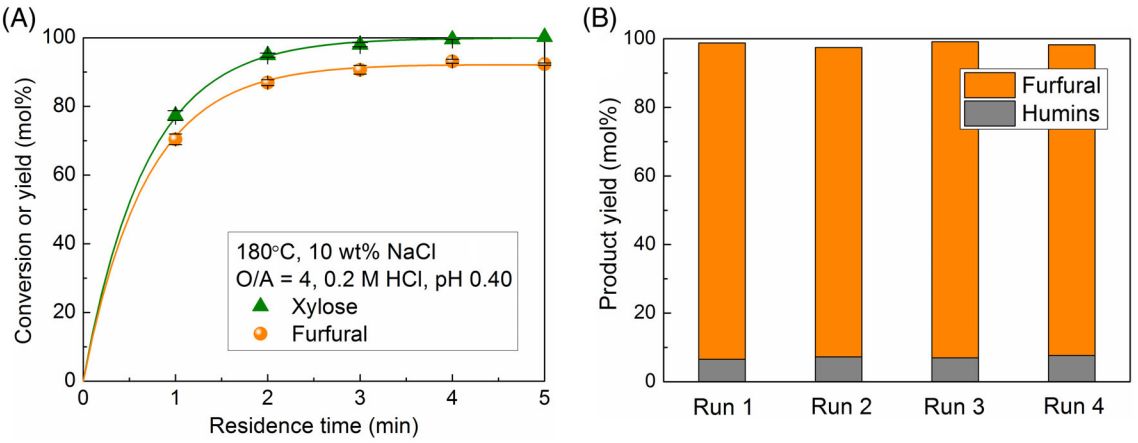

FIGURE 8 (A) Optimized xylose conversion in the slug flow capillary microreactor; (B) evaluation of the reusability of the catalytic aqueous phase containing HCl and NaCl ($\tau = 4$ min). The humin yield in (B) was estimated by assuming that it was the only source for the carbon loss. Reaction conditions: 180°C, 1 M xylose, 10 wt% NaCl, O/A = 4, 0.2 M HCl, pH 0.40 (at 20°C)

extracted into the organic phase with a complete xylose conversion, this largely facilitated recycling the catalytic aqueous phase containing HCl and NaCl by a simple phase separation (via decantation) followed by filtrating out the little amount of humins. The aqueous phase was then directly reused to prepare the fresh xylose feedstock for the following reaction run. No distinct performance loss was found after four consecutive runs (Figure 8B; each run being kept for 8 h), which proves the robustness and sustainability of the current process.

3.6 | Performance comparison with the literature

Performance of the present catalytic and microreactor system was compared with the representative literature that reported furfural synthesis from xylose in batch or flow reactors over homogeneous or heterogeneous catalysts in water-organic biphasic systems. Generally, the current microreactor affords a much higher furfural yield (e.g., $Y_{FF} = 93\%$) and space-time yield (e.g., $STY_{FF} = 36$ mol min^{-1} m^{-3}), compared with the literature work in batch ($Y_{FF} = 42\%–80\%$; $STY_{FF} = 0.03–7.5$ mol min^{-1} m^{-3}) (cf. Table S1). The lower STY_{FF} in the literature is due to the low substrate concentration, large reactor volume, batch operation mode causing a low efficiency in terms of the extended reaction time and limited furfural yield, particularly for solid catalysts (cf. the detailed discussion in Section S1 in the Supporting Information). Papaioannou et al.[23] performed xylose conversion over the H_2SO_4 catalyst in a continuous millireactor (inner diameter: 4.1 mm) at a short residence time of 2.5 min. The STY_{FF} is satisfactory (19.9 mol min^{-1} m^{-3}), but the furfural yield (ca. 56%) is moderate, possibly due to mass transfer limitation as the estimated furfural extraction rate is comparable to furfural degradation rate in their work. In addition to water, recent research attentions have also been given to utilizing other reaction media (e.g., ionic liquids,[47] polar aprotic solvents like DMSO[48] and deep eutectic solvents[49]) for xylose conversion in monophasic or biphasic systems with promising furfural yields (over 60%) obtained. However, generally, these systems are still in the stage of the preliminary lab-scale research and gave a somewhat low STY_{FF} (e.g., <10 mol min^{-1} m^{-3}) primarily due to the long reaction time (>2 h) and batch reaction mode, not to mention the higher cost and difficulty in the downstream furfural separation. In the current microreactor system (with a single 3.3 m long capillary) using water was as a cheap and green solvent, high (space time) yields of furfural and an optimized furfural production of 3.34 kg day^{-1} could be achieved, which (combined with the numbering-up approach deploying parallel reactor units) represents a promising reactor type for potential industrial applications.

4 | CONCLUSION

Furfural production from lignocellulose over homogeneous catalysts is an important industrial process with a long history, but currently still suffers from limited furfural yields (ca. 50%). To develop an efficient furfural production process, experimental and kinetic modeling studies on furfural synthesis from xylose were performed in slug flow capillary microreactors, using HCl as the catalyst and NaCl as the promotor in the aqueous phase and MIBK as the organic phase for in situ furfural extraction. An optimized furfural yield of 93% from 1 M xylose was achieved over 0.2 M HCl at 180°C and 4 min with 10 wt% NaCl addition. NaCl promotes the acidity in water and regulates the kinetics by facilitating xylose dehydration to furfural, suppressing xylose condensation, and promoting furfural degradation to humins. A comprehensive kinetic model incorporating the above effects of NaCl was developed using a first-order approach, and kinetic parameters were estimated from results of monophasic experiments in water in microreactors under varying conditions (120–180°C, the initial substrate concentration from 0.1 to 0.5 M, HCl concentration from 0.02 to 0.4 M, and NaCl addition of 0–15 wt%). The fast radial diffusion and superior heat transfer rate in monophasic microreactors allow the isothermal (high temperature) conditions and an approximate plug flow model for kinetic modeling. The quantitative correlation established between kinetic parameters and Cl^- concentrations enables the wide

model uses under other reaction conditions. In the water-MIBK biphasic system, the furfural extraction rate under slug flow was estimated to be one or two orders of magnitude higher than the rate of formation or degradation of furfural, rendering the reaction under the kinetic control, which has also been experimentally proven with varying microreactor lengths. This justifies the incorporation of equilibrium furfural extraction into the kinetic model that well predicts the experimental results of xylose conversion to furfural in slug flow microreactors. The model shows that the temperature increase enhances the furfural yield due to the higher activation energy for xylose dehydration than that for side reactions (e.g., xylose condensation and furfural degradation) leading to humins. The former side reaction is effectively suppressed by NaCl, and the latter is largely prevented in biphasic systems by the efficient furfural extraction in slug flow microreactors and high furfural partition into MIBK (further enhanced by NaCl via the salting-out effect). As a result, the furfural (space time) yield in this work is significantly higher than those reported in the literature. The upscaling of the production capacity of furfural in microreactors is also relatively straightforward by numbering up reactor units in parallel, provided that the uniform biphasic slug flow distribution is well addressed.[21] A high furfural partition into the organic phase also allowed a simple downstream phase separation and recycling of the catalytic aqueous phase which was used four times without noticeable activity loss. Thus, the continuous biphasic operation in microreactors, combined with NaCl-promoted reaction chemistry as well as the highly capable organic solvent system, holds great promises for an efficient and sustainable furfural synthesis from xylose.

ACKNOWLEDGMENTS

This research was financially supported by the University of Groningen (start-up package in the area of green chemistry and technology for Jun Yue). Wenze Guo gratefully acknowledged China Scholarship Council for the financial support (grant number 201606740069).

AUTHOR CONTRIBUTIONS

Wenze Guo: Conceptualization (supporting); data curation (equal); investigation (lead); validation (lead); writing – original draft (equal); writing – review and editing (equal). **Herman Carolus Bruining:** Investigation (supporting); validation (supporting); writing – original draft (supporting). **Hero Jan Heeres:** Supervision (supporting); writing – original draft (supporting); writing – review and editing (supporting). **Jun Yue:** Conceptualization (lead); data curation (equal); funding acquisition (lead); project administration (lead); supervision (lead); writing – original draft (equal); writing – review and editing (equal).

DATA AVAILABILITY STATEMENT

The data that support the findings of this study are available from the corresponding author upon reasonable request.

ORCID

Wenze Guo https://orcid.org/0000-0002-0543-8242
Jun Yue https://orcid.org/0000-0003-4043-0737

REFERENCES

1. Corma A, Iborra S, Velty A. Chemical routes for the transformation of biomass into chemicals. *Chem Rev*. 2007;107(6):2411-2502.
2. Huber GW, Iborra S, Corma A. Synthesis of transportation fuels from biomass: chemistry, catalysts, and engineering. *Chem Rev*. 2006;106(9):4044-4098.
3. Mika LT, Cséfalvay E, Németh Á. Catalytic conversion of carbohydrates to initial platform chemicals: chemistry and sustainability. *Chem Rev*. 2018;118(2):505-613.
4. Mäki-Arvela P, Salmi T, Holmbom B, Willför S, Murzin DY. Synthesis of sugars by hydrolysis of hemicelluloses—a review. *Chem Rev*. 2011;111(9):5638-5666.
5. Mariscal R, Maireles-Torres P, Ojeda M, Sádaba I, López Granados M. Furfural: a renewable and versatile platform molecule for the synthesis of chemicals and fuels. *Energy Environ Sci*. 2016;9(4):1144-1189.
6. Yan K, Wu G, Lafleur T, Jarvis C. Production, properties and catalytic hydrogenation of furfural to fuel additives and value-added chemicals. *Renew Sustain Energy Rev*. 2014;38:663-676.
7. Hermens JGH, Freese T, van den Berg KJ, van Gemert R, Feringa BL. A coating from nature. *Sci Adv*. 2020;6(51):eabe0026.
8. Huber GW, Chheda JN, Barrett CJ, Dumesic JA. Production of liquid alkanes by aqueous-phase processing of biomass-derived carbohydrates. *Science*. 2005;308(5727):1446-1450.
9. Danon B, Marcotullio G, de Jong W. Mechanistic and kinetic aspects of pentose dehydration towards furfural in aqueous media employing homogeneous catalysis. *Green Chem*. 2014;16(1):39-54.
10. Brownlee HJ, Miner CS. Industrial development of furfural. *Ind Eng Chem Res*. 1948;40(2):201-204.
11. Cai CM, Zhang T, Kumar R, Wyman CE. Integrated furfural production as a renewable fuel and chemical platform from lignocellulosic biomass. *J Chem Technol Biotechnol*. 2014;89(1):2-10.
12. Karinen R, Vilonen K, Niemelä M. Biorefining: heterogeneously catalyzed reactions of carbohydrates for the production of furfural and hydroxymethylfurfural. *ChemSusChem*. 2011;4(8):1002-1016.
13. da Costa Lopes AM, Morais ARC, Łukasik RM. Sustainable catalytic strategies for C5-sugars and biomass hemicellulose conversion towards furfural production. In: Fang Z, Smith JRL, Qi X, eds. *Production of Platform Chemicals from Sustainable Resources*. Springer Singapore; 2017:45-80.
14. Kruger JS, Nikolakis V, Vlachos DG. Carbohydrate dehydration using porous catalysts. *Curr Opin Chem Eng*. 2012;1(3):312-320.
15. Guo W, Heeres HJ, Yue J. Continuous synthesis of 5-hydroxymethylfurfural from glucose using a combination of $AlCl_3$ and HCl as catalyst in a biphasic slug flow capillary microreactor. *Chem Eng J*. 2020;381:122754.
16. Guo W, Zhang Z, Hacking J, Heeres HJ, Yue J. Selective fructose dehydration to 5-hydroxymethylfurfural from a fructose-glucose mixture over a sulfuric acid catalyst in a biphasic system: experimental study and kinetic modelling. *Chem Eng J*. 2021;409:128182.
17. Abdilla-Santes RM, Guo W, Bruijnincx PCA, Yue J, Deuss PJ, Heeres HJ. High-yield 5-hydroxymethylfurfural synthesis from crude sugar beet juice in a biphasic microreactor. *ChemSusChem*. 2019;12(18):4304-4312.
18. Desir P, Saha B, Vlachos DG. Ultrafast flow chemistry for the acid-catalyzed conversion of fructose. *Energy Environ Sci*. 2019;12(8):2463-2475.
19. Muranaka Y, Nakagawa H, Masaki R, Maki T, Mae K. Continuous 5-hydroxymethylfurfural production from monosaccharides in a microreactor. *Ind Eng Chem Res*. 2017;56(39):10998-11005.
20. Guo W, Kortenbach T, Qi W, Hensen E, Jan Heeres H, Yue J. Selective tandem catalysis for the synthesis of 5-hydroxymethylfurfural from glucose over in-situ phosphated titania catalysts: insights into structure, bi-functionality and performance in flow microreactors. *Appl Catal Environ*. 2022;301:120800.
21. Hommes A, Heeres HJ, Yue J. Catalytic transformation of biomass derivatives to value-added chemicals and fuels in continuous flow microreactors. *ChemCatChem*. 2019;11(19):4671-4708.

22. Sivo A, Galaverna RS, Gomes GR, Pastre JC, Vilé G. From circular synthesis to material manufacturing: advances, challenges, and future steps for using flow chemistry in novel application area. *React Chem Eng*. 2021;6(5):756-786.
23. Papaioannou M, Kleijwegt RJT, van der Schaaf J, Neira d'Angelo MF. Furfural production by continuous reactive extraction in a millireactor under the Taylor flow regime. *Ind Eng Chem Res*. 2019;58(35):16106-16115.
24. Marcotullio G, De Jong W. Chloride ions enhance furfural formation from d-xylose in dilute aqueous acidic solutions. *Green Chem*. 2010;12(10):1739-1746.
25. Marcotullio G, de Jong W. Furfural formation from d-xylose: the use of different halides in dilute aqueous acidic solutions allows for exceptionally high yields. *Carbohydr Res*. 2011;346(11):1291-1293.
26. Fulmer EI, Christensen L, Hixon R, Foster R. The production of furfural from xylose solutions by means of hydrochloric acid–sodium chloride systems. *J Phys Chem*. 1936;40(1):133-141.
27. Li Z, Luo Y, Jiang Z, Fang Q, Hu C. The promotion effect of NaCl on the conversion of xylose to furfural. *Chin J Chem*. 2020;38(2):178-184.
28. Román-Leshkov Y, Chheda JN, Dumesic JA. Phase modifiers promote efficient production of hydroxymethylfurfural from fructose. *Science*. 2006;312(5782):1933-1937.
29. Gómez Millán G, Hellsten S, King AWT, Pokki J-P, Llorca J, Sixta H. A comparative study of water-immiscible organic solvents in the production of furfural from xylose and birch hydrolysate. *J Ind Eng Chem*. 2019;72:354-363.
30. Critchfield FE, Johnson JB. Effect of neutral salts on pH of acid solutions. *Anal Chem*. 1959;31(4):570-572.
31. Weingarten R, Cho J, Conner JWC, Huber GW. Kinetics of furfural production by dehydration of xylose in a biphasic reactor with microwave heating. *Green Chem*. 2010;12(8):1423-1429.
32. Krzelj V, Ferreira Liberal J, Papaioannou M, van der Schaaf J, Neira d'Angelo MF. Kinetic model of xylose dehydration for a wide range of sulfuric acid concentrations. *Ind Eng Chem Res*. 2020;59(26):11991-12003.
33. Lamminpää K, Ahola J, Tanskanen J. Kinetics of xylose dehydration into furfural in formic acid. *Ind Eng Chem Res*. 2012;51(18):6297-6303.
34. Dussan K, Girisuta B, Lopes M, Leahy JJ, Hayes MHB. Conversion of hemicellulose sugars catalyzed by formic acid: kinetics of the dehydration of D-xylose, L-arabinose, and D-glucose. *ChemSusChem*. 2015;8(8):1411-1428.
35. Nagy KD, Shen B, Jamison TF, Jensen KF. Mixing and dispersion in small-scale flow systems. *Org Process Res Dev*. 2012;16(5):976-981.
36. Silvester LF, Pitzer KS. Thermodynamics of electrolytes. 8. High-temperature properties, including enthalpy and heat capacity, with application to sodium chloride. *J Phys Chem*. 1977;81(19):1822-1828.
37. Li Z, Luo Y, Jiang Z, Fang Q, Hu C. The promotion effect of NaCl on the conversion of xylose to furfural. *Chin J Chem*. 2019;37:178-184.
38. Mellmer MA, Sanpitakseree C, Demir B, et al. Effects of chloride ions in acid-catalyzed biomass dehydration reactions in polar aprotic solvents. *Nat Commun*. 2019;10(1):1132.
39. Huang J, He C, Wu L, Tong H. Thermal degradation reaction mechanism of xylose: a DFT study. *Chem Phys Lett*. 2016;658:114-124.
40. van Baten JM, Krishna R. CFD simulations of mass transfer from Taylor bubbles rising in circular capillaries. *Chem Eng Sci*. 2004;59(12):2535-2545.
41. Hommes A, de Wit T, Euverink GJW, Yue J. Enzymatic biodiesel synthesis by the biphasic esterification of oleic acid and 1-butanol in microreactors. *Ind Eng Chem Res*. 2019;58:(34):15432-15444. https://doi.org/10.1021/acs.iecr.9b02693
42. Kashid MN, Gerlach I, Goetz S, et al. Internal circulation within the liquid slugs of a liquid−liquid slug-flow capillary microreactor. *Ind Eng Chem Res*. 2005;44(14):5003-5010.
43. Trachsel F, Günther A, Khan S, Jensen KF. Measurement of residence time distribution in microfluidic systems. *Chem Eng Sci*. 2005;60(21):5729-5737.
44. Swatloski RP, Spear SK, Holbrey JD, Rogers RD. Dissolution of cellose with ionic liquids. *J Am Chem Soc*. 2002;124(18):4974-4975.
45. Liu Z, Zhang C, Liu R, et al. Dissolution of cellobiose in the aqueous solutions of chloride salts: Hofmeister series consideration. *Cellulose*. 2016;23(1):295-305.
46. Sánchez R, Hernández C, Keresztury G. Structural analysis of acid catalysed furfuraldehyde resins by thermal degradation techniques. *Eur Polym J*. 1994;30(1):43-50.
47. Peleteiro S, Rivas S, Alonso JL, Santos V, Parajó JC. Furfural production using ionic liquids: a review. *Bioresour Technol*. 2016;202:181-191.
48. Lam E, Majid E, Leung ACW, Chong JH, Mahmoud KA, Luong JHT. Synthesis of furfural from xylose by heterogeneous and reusable Nafion catalysts. *ChemSusChem*. 2011;4(4):535-541.
49. Zhang L, Yu H. Conversion of xylan and xylose into furfural in biorenewable deep eutectic solvent with trivalent metal chloride added. *BioResources*. 2013;8(4):6014-6025.

SUPPORTING INFORMATION

Additional supporting information may be found in the online version of the article at the publisher's website.

How to cite this article: Guo W, Bruining HC, Heeres HJ, Yue J. Efficient synthesis of furfural from xylose over HCl catalyst in slug flow microreactors promoted by NaCl addition. *AIChE J*. 2022;68(5):e17606. doi:10.1002/aic.17606